

# Journal of Biomedical Optics

BiomedicalOptics.SPIEDigitalLibrary.org

## Optical properties of animal tissues in the wavelength range from 350 to 2600 nm

Serafima A. Filatova  
Ivan A. Shcherbakov  
Vladimir B. Tsvetkov

**SPIE.**

Serafima A. Filatova, Ivan A. Shcherbakov, Vladimir B. Tsvetkov, "Optical properties of animal tissues in the wavelength range from 350 to 2600 nm," *J. Biomed. Opt.* **22**(3), 035009 (2017), doi: 10.1117/1.JBO.22.3.035009.

# Optical properties of animal tissues in the wavelength range from 350 to 2600 nm

Serafima A. Filatova,<sup>a,b,\*</sup> Ivan A. Shcherbakov,<sup>a</sup> and Vladimir B. Tsvetkov<sup>a,c</sup>

<sup>a</sup>General Physics Institute of Russian Academy of Sciences, Moscow, Russia

<sup>b</sup>Ulyanovsk State University, Laboratory of Quantum Electronic and Optoelectronic, Ulyanovsk, Russia

<sup>c</sup>National Research Nuclear University MEPhI, Laboratory of Laser Thermonuclear Fusion, Moscow, Russia

**Abstract.** The optical properties of different cow and pig biological tissues such as skeletal muscle, adipose, spinal cord, and dura mater of the spinal cord were investigated in the spectral range of 350 to 2600 nm. The measurements were carried out by a commercially available spectrophotometer SHIMADZU UV 3101PC. The wavelength dependence on the scattering coefficient has been observed to follow a power-law decay for skeletal muscle and dura mater of spinal cord. The influence of time delay between the sample preparation and measuring of transmittance spectra on the data reasonableness was reviewed. The conclusion about the benefits of 2- $\mu\text{m}$  lasers application in surgery is given for the tissue types listed above. © 2017 Society of Photo-Optical Instrumentation Engineers (SPIE) [DOI: [10.1117/1.JBO.22.3.035009](https://doi.org/10.1117/1.JBO.22.3.035009)]

**Keywords:** optical properties of biological tissues; absorption coefficient; extinction coefficient; skeletal muscle tissue; adipose tissue; spinal cord tissue; dura mater of spinal cord.

Paper 160724R received Oct. 26, 2016; accepted for publication Mar. 7, 2017; published online Mar. 22, 2017.

## 1 Introduction

Active usage of laser technologies in various fields of medicine (diagnosis,<sup>1</sup> therapy,<sup>2</sup> and surgery<sup>3</sup>) favors the study of the optical properties of biological tissues. A particular line of research concentrates on the determination of the laser radiation propagation inside the tissue. The result of the laser radiation impact on biological tissues depends on their optical and thermal characteristics. First of all, it is necessary to have accurate information about the value of water content, absorption coefficient, scattering coefficient, and refractive index for various biological tissues,<sup>4</sup> as well as their thermal conductivity. The information about the biological tissue optical properties allows accurate prediction of the radiation distribution in the tissue. It helps to determine absorbed dose of laser radiation and to predict tissue zone of any changes and necrosis. Nowadays, there are plenty of the articles devoted to the optical properties of biological tissues.<sup>5,6</sup> However, the majority of these investigations was made for specific applications; therefore, there were different methods of sample preparation. This leads to the difference in the findings. Furthermore, results of *in vitro* investigation of biological tissues transmittance may depend on the time delay between the sample preparation and measurements.

The publications are mostly devoted to the investigation of biological tissues characteristics in the visible and short-wave infrared spectral range (250 to 1100 nm). However, measurements in this spectral range do not provide the information for application of lasers with wavelength of 1.5 and 2  $\mu\text{m}$ . It is interesting to study and get more information about optical properties of various biological tissues in the range of 1.1 to 2.5  $\mu\text{m}$ <sup>5,6</sup> because there are absorption lines of water,<sup>7</sup> lipids,<sup>8,9</sup> and collagen<sup>10</sup> in this range. Furthermore, published data about the values of absorption coefficients of various biological tissues

are very different. Therefore, we need to know exact data about tissue absorption characteristics for proper study of the applicability of 2- $\mu\text{m}$  lasers in medicine or the impact on the tissue under investigation.

We present the investigation of biological tissue absorption spectra in the range of 1.1 to 2.6  $\mu\text{m}$  while most of published articles are devoted to studies in the near infrared range. All the measurements were made in the spectral range of 0.35 to 2.6  $\mu\text{m}$  for comparison with known data. Also, in published articles, we did not find any information about the influence of the time delay between the sample preparation and the measurements to the spectral characteristics of the tissue. Thus, measurements were carried out immediately after sample preparation and sequentially in 10 min intervals between measurements. Conditions of measurements for all samples were similar. In addition, in this study we investigated different types of the same tissues to compare the transmittance in the case of different size and density of the muscle fibers and the fat content. In the measuring process, we used unpolarized light because the final goal of our study was to obtain the data for predicting the results of laser radiation impact. In this case, the laser radiation is unpolarized due to the optical fiber delivery.

## 2 Materials and Methods

We investigated cow and pig skeletal muscle tissues, adipose tissues, as well as pig spinal cord and dura mater of the spinal cord. We selected the biological tissues for the study because of the necessity to compare the tissues with various extents of ordered scattering centers and with different water content. We took the samples of muscle tissue from the different skeletal muscles to compare the transmittance in the case of different size and density of the muscle fibers and the fat content. All biological tissue samples were bought on the open market as

\*Address all correspondence to: Serafima A. Filatova, E-mail: [films2910@gmail.com](mailto:films2910@gmail.com)

parts of dead animals, so we do not use live animals and do not remove tissue samples from live animals. General Physics Institute, where the experiments were conducted, approves this.

The transmittance measurements were done at room temperature *in vitro*, 5 to 6 h after biopsy. The sizes of the samples were about  $15 \times 15 \text{ mm}^2$ . All the samples were mounted on a specially designed cell between two identical optical windows (Fig. 1) made of fused silica. The compression force was less than 10 N. Deformation of the samples was less than 0.1 mm, so the optical characteristics of biological tissues were not changed.<sup>11</sup> The cell was designed in such a way that in the absence of the sample the gap between glass plates and the gap between the optical window holders were equal to zero ( $\Delta = 0$ ). This allowed us to determine the sample thickness by measuring the gap value between the window holders. The gap value was measured several times over the perimeter of the holders with an accuracy of 0.05 mm. The average value was taken as the sample thickness.

The transmittance of biological tissue is determined both by light absorption and scattering. The contribution of different processes (single and multiple scattering, scattering characteristics, etc) is determined by tissues morphology because the size of cells and cells' structural elements are in the range of several tens of nanometers to hundreds of micrometers.<sup>12,13</sup> Various methods may be used for complete characterization of light transmittance process in biological tissue (for instance, Ref. 14).

The spectrophotometric method could be employed while using the conventional equipment. Basic models of light propagation in biological tissues are described in terms of radiation transport in a random inhomogeneous media. However, in the case of thin samples with high absorption coefficient and a relatively small light scattering, we can put into practice the semi-empirical equation, while using a continuous wave collimated probe beam<sup>14,15</sup>

$$T_c(\lambda) = x_1 \exp[-\mu_t(\lambda) * L(\lambda)x_2], \quad (1)$$

where  $L(\lambda)$  is the average length of the full path of photons (including scattering),  $\mu_t(\lambda) = \mu_a(\lambda) + \mu_s(\lambda)$  is the extinction coefficient (attenuation),  $\mu_a$  is the absorption coefficient,  $\mu_s$  is the scattering coefficient,  $x_1$  is the parameter that takes into account the contribution of multiply scattered, but not absorbed photons, that did not reach the detector, as well as the measurement geometry, and  $x_2$  is the coefficient that compensates for an error in thickness measurement and inaccuracy in determination of the scattering coefficient  $\mu_s$ . This equation defines a probe beam transmittance both when using an integrating sphere or not (at different correction functions  $x_1$ ).

Effective light penetration depth into a biological tissue subject to light scattering is determined by the expression<sup>14</sup>

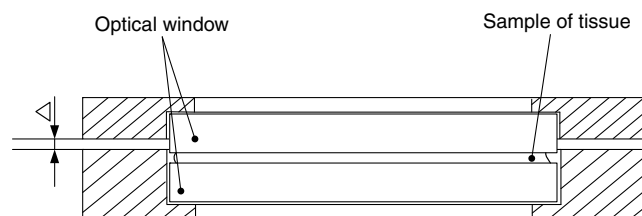


**Fig. 1** The scheme of the cell for measuring biological tissues transmittance spectra.

$$\mu_{\text{eff}} = \sqrt{3\mu_a[\mu_a + \mu_s(1 - g)]}, \quad (2)$$

where  $\mu_s$  is the scattering coefficient and  $g$  is the anisotropy factor. The measuring method of collimated light beam transmittance provides less information than the data obtained with the simultaneous measurement of light transmittance and scattering. Nevertheless, for thin layers, this method allows for the accurate determination of the absorption coefficient of biological tissues.

In our study, the thickness of investigated samples was 0.15 to 1.8 mm. On one hand, it allowed us to measure the transmittance spectrum in the spectral ranges of water absorption, and conversely it could reduce light scattering effect on the results. Thus, we have measured transmittance of continuous wave light source with a collimated probe beam without using an integrating sphere. The contribution of scattering to extinction coefficient was not measured experimentally but was estimated while using the transmittance data.

Transmittance spectra were measured in the spectral range 350 to 2600 nm when using a spectrophotometer SHIMADZU UV 3101PC. The spectral width of the slit was 3 nm, scan speed  $200 \text{ nm} \times \text{min}^{-1}$ . The solid angle of collection was 0.5 sr, so the probability of catching the multiply scattered light by the detector is small. Time measuring of transmittance spectrum in the whole spectral range was about 12 min. Data processing was performed after measurements for the determination of the samples' absorption spectra. We used the expression (1), in which  $x_1(\lambda)$  has taken into account the spectral dependence of transmittance of measuring cell windows and the contact between cell window and the sample.

In sample preparation, the part of tissue cells is destroyed and tissue fluid is leaked. The measurement of one sample was repeated several times with 10 min intervals to observe changes of transmittance spectrum over time. As all the soft biological tissues consist of 70% to 80% water, the biological tissues absorption spectra were compared with water absorption spectrum.

### 3 Results and Discussion

In the study, we were interested particularly in obtaining the data of biological tissues absorption in the range of 1900 to 2200 nm. However, the transmittance spectra strongly depend on scattering in biological tissue samples as well, so the measurements were carried out over a wide spectral range of 350 to 2600 nm to estimate the contribution of scattering to the transmittance and to compare results with the known data of light absorption in biological tissues, measured in visible and short-wave infrared spectral range (250 to 1100 nm).

First of all, we were interested in studying the influence of optical windows wetting due to tissue fluid leakage from the destroyed cells on the measurement results. Measurements were carried out immediately after sample preparation ( $t_0$ ), and sequentially, with 10 min intervals between measurements. The same measurements were carried out for all types of samples.

Figure 2(a) shows the raw transmittance spectra in time obtained by spectrophotometer. Figure 2(b) shows the transmittance spectra in time with compensation of glass slides transmittance, between which the sample of biological tissue is fixed. These spectra were obtained by

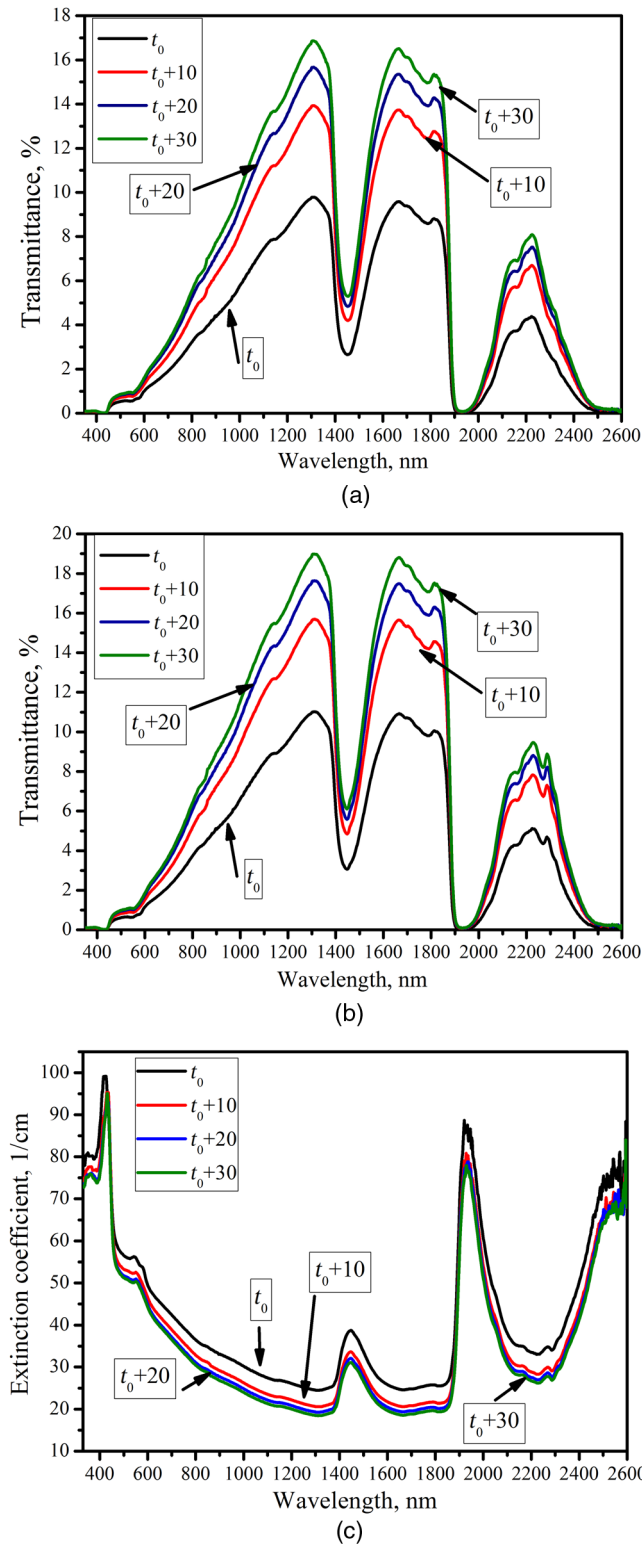


**Fig. 2** (a) The raw transmittance spectra in time for MN03 sample of cow trapezius muscle; (b) the transmittance spectra in time for MN03 sample of cow trapezius muscle with compensation of glass slides transmittance; (c) the extinction spectra of the MN03 sample of cow trapezius muscle. The transmittance spectra were measured with 10 min intervals between measurements.

$$\mu_t(\lambda) = \frac{-\ln\left(\frac{T_c}{x_1}\right)}{L}, \quad (3)$$

in which  $x_1(\lambda)$  has taken into account the spectral dependence of glass slides transmittance and the contact between glass slides and the sample. Figure 2(c) shows the curves of the spectral dependence of extinction coefficient for the MN03 sample of cow trapezius muscle. Spectra were obtained for the sample being cut from the trapezius muscle of cow (sample MN03, 0.9 mm thickness).

The curves in Fig. 2 show that transmittance of the cell is increased with the rise in time delay between the sample preparation and the measurement. However, the spectra seem to be the similar figures without changes in the values of extinction coefficient in absorption lines. Transmittance spectra demonstrate small changes after 20 min of exposure. This may be due to the fact that tissue fluids that run out from the damaged intercellular connections wet the glass slides of our measuring cell more and more. The wetting influences the reflection coefficient from the wet glass slides (diminishing the reflection coefficient). The water content in the tissues was not changed, whereas only the structures were cut. Similar results were obtained for the other tissue samples. Thus, it is required to wait about 30 min after sample preparation for proper measurements.

The next issue was to single out the absorption spectra from the extinction spectra by taking into account the light scattering in the sample. Biological tissues are optically inhomogeneous absorbing media with an average refractive index greater than air. The optical light scattering in biological tissues can be explained by two concepts (see Ref. 12). In one case, the light scattering in medium with continual but spatially inhomogeneous refractive index is considered. In another case, the light scattering by particles with refractive index different from the refractive index of medium is considered. In the second case, the scattering can be described by the formalism of the Mie theory, while implying that ideal spheres of a certain size are in a homogeneous medium. The presence of scattering centers with different sizes and shapes in biological tissue may complicate understanding of the scattering mechanisms. However, in our case, it is interesting to obtain just the absorption spectrum, and we do not discuss the light scattering mechanisms. Spectral dependence of the scattering coefficient for many types of tissues is the sum of Rayleigh scattering in the short-wavelength range and Mie scattering in the long-wavelength range (see Refs. 6 and 16). However, for a number of biological tissues, good approximation can be achieved using a power-law decay function  $\mu_s \propto \lambda^{-h}$  (see Refs. 6, 16, and 17). In the experimental data processing, we started from the assumption that Mie scattering plays a greater role in the UV and visible spectral ranges than in the IR range, and the general rise of the absorption spectrum due to water absorption starts at  $\sim 1050$  nm.<sup>7</sup> The result of this approach is shown in Fig. 3 for a 0.9-mm-thick sample cut from a cow trapezius muscle.

One can see that the power function describes the scattering losses rather well in the visible spectral range. For approximation of the spectral dependence of the scattering coefficient, we used the expression

$$\mu_s = K\lambda^{-h}, \quad (4)$$

similar to the equation used in Ref. 6.

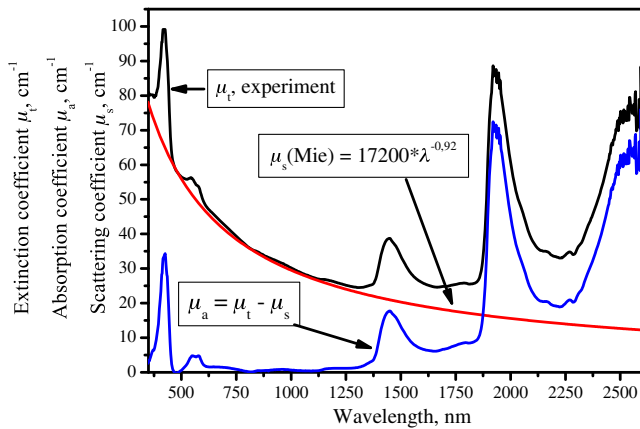


**Fig. 3** Spectral dependence of the extinction coefficient, the estimated scattering coefficient, and the absorption coefficient for the MN03 sample of cow trapezius muscle.

### 3.1 Absorption Spectra of Cow and Pig Skeletal Muscle Tissues

In total, we used 12 samples of cow and pig skeletal muscle tissues (“hard” and “soft” meat with different density of muscle fibers and various fat contents) of different thickness for *in vitro* transmittance spectra measurements. Figure 4 shows the absorption spectra of cow skeletal muscle tissue samples—trapezius (MN03, sample thickness was 0.9 mm) and longissimus dorsi-muscle (MR01, sample thickness was 1 mm).

As we can see from the graphs, the position of the main absorption lines coincides for all the samples. The value of trapezius muscle absorption coefficient at the wavelengths of  $\lambda \approx 1450$ , 1930, and 2500 nm is approximately two times higher than the values obtained for the longissimus dorsi-muscle tissue. These wavelengths correspond to absorption of water (O-H group), indicating the high water content in the sample being cut from the trapezius muscle. The value of absorption coefficient in the range of about 970 and 1200 nm is also different, and it is also different from the water absorption data. This effect may be related to the fact that in the range of about 970 and 1200 nm there are superposition of absorption lines originated

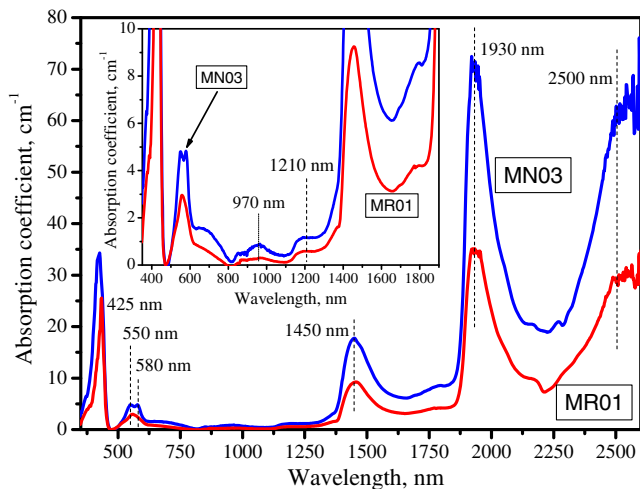


**Fig. 4** Absorption spectra of cow skeletal muscle samples: trapezius (sample MN03) and the longissimus dorsi-muscle (sample MR01). The inset shows the absorption spectra in an enlarged scale.

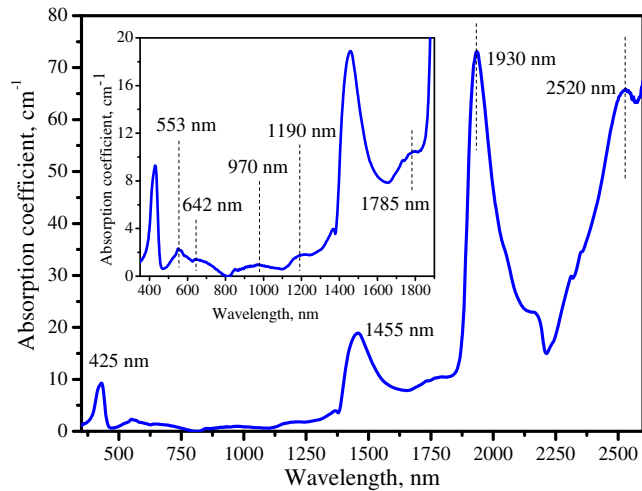


**Fig. 5** Absorption spectra of the MLB02 sample of the pig muscle (longissimus dorsi-muscle) 0.5 mm thick. The inset shows the absorption spectrum in an enlarged scale.

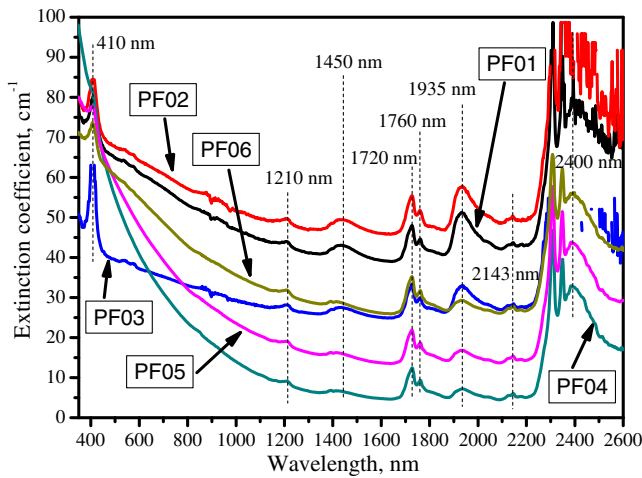
from water O-H groups (970 and 1180 nm<sup>6</sup>) and C-H groups (920, 1050, and 1210 nm, connected with an absorption of lipids and collagen from the muscle tissue, see for example Ref. 5). We can also see the difference in absorption spectra at  $\lambda \approx 425$ , 550, and 580 nm, connected with the hemoglobin absorption.<sup>5</sup>

Figure 5 demonstrates the absorption spectra of the pig muscle tissue (the longissimus dorsi-muscle, sample MLB02 0.5 mm thick).

As we can see, the main absorption lines in cow and pig muscle tissues coincide. The value of the absorption coefficient at wavelengths corresponding to the OH-groups (water absorption) shows that water content in the pig longissimus dorsi-muscle tissue is almost the same as in the cow trapezius muscle and is about two times higher than in the cow longissimus dorsi-muscle. For samples of the pig longissimus dorsi-muscle and cow trapezius muscle, the average value of absorption coefficients are  $\alpha = 13 \pm 2 \text{ cm}^{-1}$  at  $\lambda \approx 1450$  nm and  $\alpha = 58 \pm 5 \text{ cm}^{-1}$  at  $\lambda \approx 1930$  nm. Standard deviations were obtained by studying the whole set of sample results (eight pieces). In the case of cow and pig muscle study, significant difference in the absorption lines belonging to the actual biological tissue was not obtained, with the exception of water content. It is possible that the similarity of the spectra is explained by lipid and collagen absorption lines being masked by water absorption lines. Comparison of data in this study and data presented in Ref. 18 shows a good agreement between them in the spectral range of 620 to 1000 nm, as well as in Ref. 19 in the spectral range of 600 to 950 nm.

### 3.2 Extinction Coefficient Spectra of Pig Adipose Tissue

We used six samples cut from the pig longissimus dorsi-muscle for *in vitro* measurements of subcutaneous adipose tissue transmission spectra. Samples were cut in the following way: three samples (PF01-PF03) were cut near the skin (the increasing of the sample number shows the deepening into the fat tissue from the skin) and three samples (PF04-PF06) were cut near the muscle (increase sample number also shows getting deeper into the fat tissue from the muscle). Sample thickness was varied in the range of 0.3 to 1.8 mm. Transmission spectra of adipose



**Fig. 6** Extinction coefficient spectra of pig adipose tissue. The samples were cut from pig adipose tissue in the area of the longissimus dorsi-muscle. PF01-PF03 samples were cut closer to the skin, and PF04-PF06 samples were closer to the muscle.

tissue samples also showed the dependence of delay time between the sample preparation and measurements, so transmittance measurements were done after 30 min exposure. Figure 6 shows the extinction spectra in the range of 350 to 2600 nm of the pig adipose tissue samples with different thickness.

These overview extinction spectra clearly display the difference in extinction coefficient at wavelengths of  $\lambda \approx 410$ , 1450, and 1935 nm, depending on the location of the sample cut. In turn, the bands at 1210, 1720, 1760, 2143, and 2400 nm are almost identical in all the investigated samples of pig adipose tissue.

One can see that water content (the absorption coefficient at wavelength of 1935 nm) in the samples cut close to the skin (samples 1 to 3) is higher than in samples cut far from the skin (samples 4 to 6). Furthermore, the scattering in subcutaneous adipose tissue samples cannot be described in a proper way by a simple approximation while using the Mie function [Eq. (4)], or more complex function that takes into account both Rayleigh scattering and Mie scattering (see Ref. 16). Apparently, the scattering centers in the subcutaneous adipose tissue have a wide range of sizes and may be heterogeneously distributed. It should be noted that Mie approximation demonstrates better results for the samples that cut closer to the muscle. Perhaps the samples cut near the skin possess higher inhomogeneity, i.e., a large number of different centers (or fluctuations of refractive index) are available. For appropriate description of light scattering in biological tissue, we need to know the scattering centers sizes and their refractive indexes (structural elements of biological tissue). It has no physical sense to make the approximation of the “scattering base” by any function without creation of a proper conception.

The absorption band at 1210 nm is a combination of the absorption bands of water and lipids located at 1197 and 1212 nm, respectively.<sup>20</sup> Absorption bands at 1450 nm are the superposition of vibrational absorption bands of O-H groups (water<sup>7</sup>) and C-H groups (cholesterol, lipids, and collagen<sup>5,20,21</sup>). The group of absorption bands at 1720 and 1760 nm corresponds to absorption of cholesterol and other types of fatty alcohols (or long-chain alcohols)<sup>5</sup> as described in Refs. 20 and 21. Absorption band in the range of 1935 nm corresponds to the water absorption.<sup>5</sup> Water content in samples near the skin

(samples 1 to 3) is higher than in samples cut far from the skin (samples 4 to 6). Perhaps, the observed changes in absorption coefficient at 1450 and 1935 nm can be explained by the change of water content in different areas of subcutaneous fat, while lipids and collagen average content remains the same. Perhaps the absorption bands in the range of 2400 nm also correspond to cholesterol, lipids, and collagen.<sup>21</sup> It is not correct to compare our data of extinction coefficient with the data of absorption coefficient of the other groups for adipose tissues. But it may be noted that the main absorption lines in our spectra are coincide with absorption lines obtained for human and rat adipose tissues calculated using IAD method after spectra measurements by spectrophotometer CARY-2415 (Varian, Australia) with an integrating sphere (Refs. 6 and 20).

We did not observe the similar dependence of the transmission spectra on the location of cutting the sample for skeletal muscles. For the detailed explanation of this effect, it will be necessary to make the thorough analysis of the accordance of observed absorption lines to the components of pig adipose tissue. This will be the subject of a separate study.

### 3.3 Extinction Coefficient Spectra of Pig Spinal Cord Tissue and Dura Mater of Spinal Cord

Transmission spectra of pig spinal cord tissue also show the dependence of the time delay between the sample preparation and the measurements. So the transmittance measurements were also carried out after 30 min of exposure.

The extinction coefficient spectrum of the pig spinal cord is shown in Fig. 7. Scattering in the pig spinal cord tissue samples as well as in subcutaneous adipose tissue cannot be correctly described by a simple approximation with the use of the Mie function [Eq. (4)] or while using a more complex function that takes into account both Rayleigh scattering and Mie scattering. It seems that the scattering centers in this tissue have a wide range of sizes and may possess an inhomogeneous volume distribution that is the same as for a fatty tissue. Therefore, the approximation of a “scattering base” was not done. Water absorption bands (1450 and 1930 nm) are clearly seen in the extinction coefficient spectrum of the pig spinal cord. There

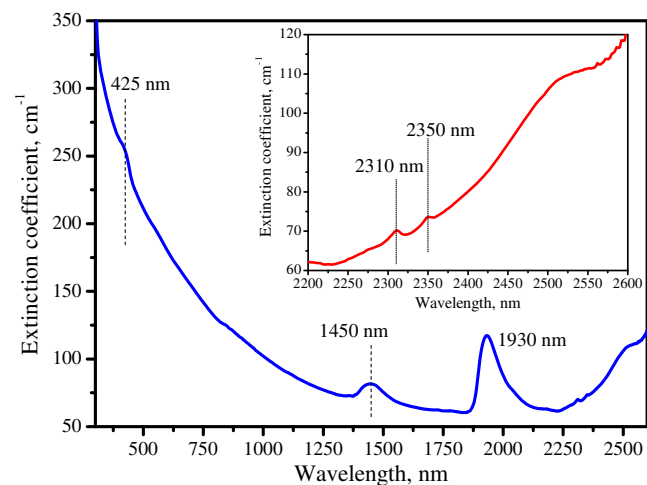


**Fig. 7** The extinction coefficient spectrum of a pig spinal cord. Sample thickness is 0.15 mm. The inset shows the weak absorption bands near 2350 nm.

are also the weak absorption bands of hemoglobin (425 nm) and apparently, cholesterol, lipids, and collagen (2350 nm).

It should be noted that the used method of simple measurements of biological tissue transmittance using a standard spectrophotometer provides accurate data on the absorption lines position and absorption coefficient value in the case of using a thin samples. Thus, in the spinal cord extinction spectrum (Fig. 7), we can clearly observe weak absorption bands (e. g.,  $\mu_a = 1.5 \text{ cm}^{-1}$  at 2310 nm) together with strong absorption at 1930 nm ( $\mu_a = 56 \text{ cm}^{-1}$ ). The accuracy of absorption coefficient determination was  $\Delta\mu_a = 0.1 \text{ cm}^{-1}$ .

Additionally, the muscle tissue of the dura mater of the spinal cord is formed mostly by collagen fibers. Therefore, we can expect that the contribution of light scattering coefficient into dura mater extinction coefficient will be less than in adipose tissue and in spinal cord due to approximately the same size and orientation of the scattering centers. Figure 8 shows the absorption spectrum of a pig dura mater of spinal cord (sample thickness is 0.45 mm).

One can see that the scattering is well approximated by Mie expression (4) in the assumption of the same size of scattering

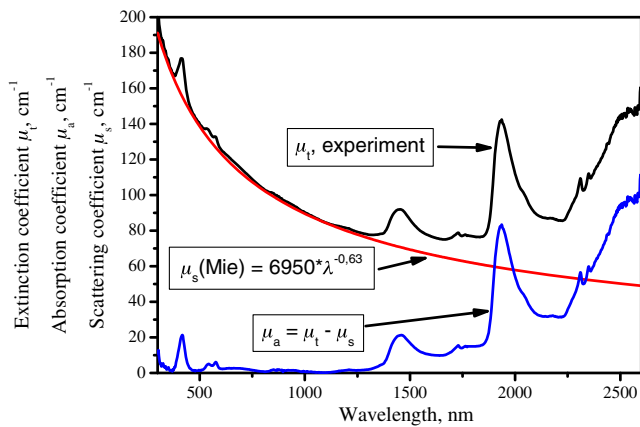


**Fig. 8** Dependence of the spectral extinction coefficient of pig dura mater (sample DM03) and estimated scattering and absorption coefficients.

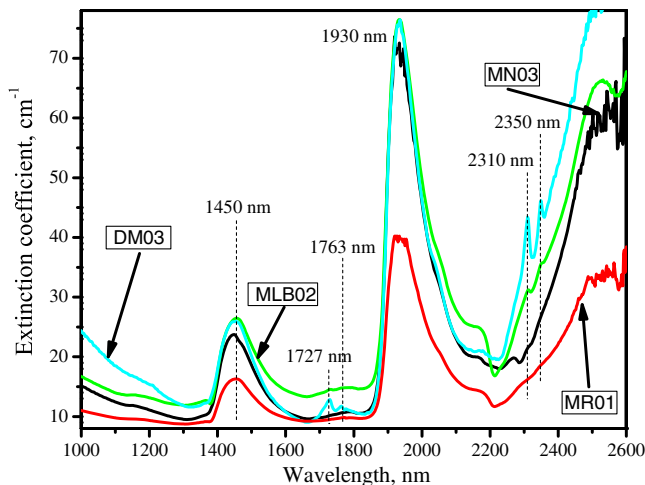


**Fig. 9** Combination of cow (MR01, MN03) and pig (MLB02) muscle extinction spectra and a pig dura mater of spinal cord (DM03). All spectra are in the same scale and superimposed with a shift on the Y axis.

centers. Generally, the absorption spectrum of pig dura mater of the spinal cord is quite similar to the muscle tissue absorption spectra (see Fig. 9). It is an expected result because both tissues are composed of the same structural elements (with different percentage).

### 3.4 Comparison and Analysis of Obtained Spectra

One can see that the main absorption bands in skeletal muscle tissues and in dura mater are determined by water absorption (bands at 1450 and 1930 nm). The absorption spectra of cow and pig muscles are almost identical (as was mentioned), but they may differ by water content. Also, in a pig muscle tissue absorption spectra, there is additional absorption at 2310 and 2350 nm. It may correspond to cholesterol, lipids, and collagen absorption. Absorption bands of pig dura mater at 1727, 1763, 2310, and 2350 nm stood out against the main spectrum. These absorption bands are also characteristic for adipose tissue absorption and correspond to absorption of different types of lipids (including cholesterol).<sup>5,22,23</sup>

In spite of the spectral function of the light scattering in the pig spinal cord being similar to adipose tissues, the absorption spectrum of pig spinal cord is much more similar to absorption in skeletal muscle tissues (Fig. 10). It is seen that water makes the main contribution to light absorption in the spinal cord (bands at 1450 and 1930 nm) unlike in the adipose tissue.

As the light absorption in animals and human tissues have many similar characteristics,<sup>24</sup> we can say that for surgical laser impact on skeletal muscle and adipose tissues as well as spinal cord and dura mater, it is more preferable to use the water absorption bands. It is not possible to find the wavelength that could provide a selective impact on biological tissues listed above without damage of surrounding tissues. Therefore, we consider that the main task is the selection of the laser radiation wavelength that would have the least undesirable impact on both the target and the surrounding tissues. In this case, one of the optimal spectral ranges of exposure is the range of 1900 to 2200 nm, in which laser radiation can be obtained by thulium and holmium lasers while using both crystal and glass active medium (including fiber lasers). It is possible to change the lasing wavelength in the range of 1800 to 2100 nm for thulium

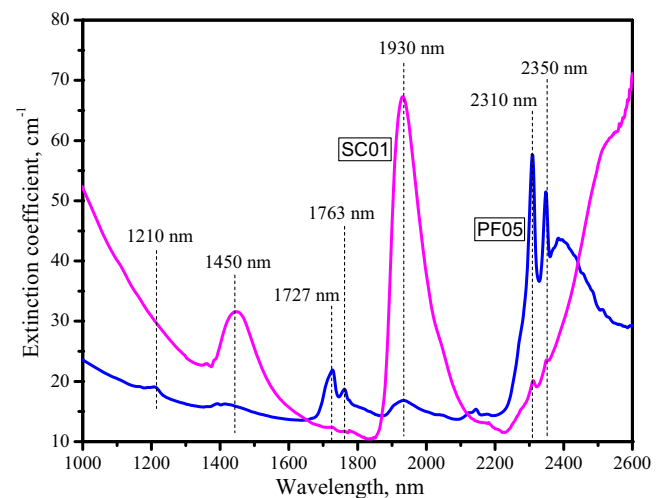


**Fig. 10** Combination of the extinction spectra of pig spinal cord (sample SC01) and pig adipose tissue (sample PF05). All spectra are in the same scale and superimposed with a shift on the Y axis.

fiber lasers (see Ref. 25) and in the range of 2030 to 2210 nm for holmium fiber lasers (see Refs. 26 and 27). This gives the possibility of accurately choosing a wavelength for a particular operation. As in this spectral range the absorption coefficient is varied from a fraction of a unit to tens of  $\text{cm}^{-1}$ , it is possible to choose the laser wavelength for weakly absorbing (adipose tissue) and high absorbing (skeletal muscles, spinal cord, and dura mater) tissues. Application of 2- $\mu\text{m}$  lasers seems to be preferable in contrast to 1.5- $\mu\text{m}$  lasers not only in terms of higher absorption coefficient in biological tissues but also in terms of significantly less light scattering coefficient.

#### 4 Conclusions

Extinction and absorption spectra of various biological tissues in the range of 330 to 2600 nm were obtained. The influence of time delay between the sample preparation and measuring of transmittance spectra on the data reasonableness was reviewed. It is shown that measurements of light absorption and scattering in biological tissue should be carried out after 30 min of sample preparation to obtain reasonable data. It comes due to complete wetting of the cell windows surface. Also, different types of the same tissues were investigated for comparing the transmittance in the case of different size and density of the muscle fibers and the fat content. Absorption spectra of various skeletal muscle tissues are very similar both by absorption bands position and the value of absorption coefficient (including the observed similarity for different animals—pig and cow) and are similar to absorption in pig spinal cord and dura mater tissue samples. Absorption of adipose tissue is quite different from all the other investigated tissues. The conclusion about benefits of 2- $\mu\text{m}$  lasers application in surgery is given for the tissue types listed above.

#### Disclosures

No conflicts of interest, financial or otherwise, are declared by the authors.

#### Acknowledgments

The research was supported by the Russian Academy of Sciences in the frames of the program for basic research “Basic and application problems of photonics and the physics of novel optical materials” (Project No. I.25Π) and by the Ministry of Education and Science of the Russian Federation (Project No. 14.Z50.31.0015).

#### References

1. Y. Nakai et al., “Confocal laser endomicroscopy in gastrointestinal and pancreaticobiliary diseases,” *Digestive Endoscopy* **26**(S1), 86–94 (2014).
2. E. Cinotti et al., “Laser photodynamic treatment for in situ squamous cell carcinoma of the glans monitored by reflectance confocal microscopy,” *Australas. J. Dermatol.* **55**(1), 72–74 (2014).
3. C. L. Hoy et al., “Clinical ultrafast laser surgery: recent advances and future directions,” *IEEE J. Sel. Top. Quantum Electron.* **20**(2), 242–255 (2014).
4. A. N. Bashkatov, E. A. Genina, and V. V. Tuchin, “Optical properties of skin, subcutaneous, and muscle tissues: a review,” *J. Innovative Opt. Health Sci.* **4**(01), 9–38 (2011).
5. R. H. Wilson et al., “Review of short-wave infrared spectroscopy and imaging methods for biological tissue characterization,” *J. Biomed. Opt.* **20**(3), 030901 (2015).

6. A. N. Bashkatov et al., “Optical properties of human skin, subcutaneous and mucous tissues in the wavelength range from 400 to 2000 nm,” *J. Phys. D* **38**(15), 2543 (2005).
7. G. M. Hale and M. R. Querry, “Optical constants of water in the 200 nm to 200  $\mu\text{m}$  wavelength region,” *Appl. Opt.* **12**(3), 555–563 (1973).
8. R. L. van Veen et al., “Determination of VIS-NIR absorption coefficients of mammalian fat, with time- and spatially resolved diffuse reflectance and transmission spectroscopy,” in *Biomedical Topical Meeting (p. SF4)* (2004).
9. G. B. Althuler, R. R. Anderson, and D. Manstein, “Method and apparatus for the selective targeting of lipid-rich tissue,” U. S. Patent No. 6,605,080 (2003).
10. R. Nachabé et al., “Diagnosis of breast cancer using diffuse optical spectroscopy from 500 to 1600 nm: comparison of classification methods,” *J. Biomed. Opt.* **16**(8), 087010 (2011).
11. G. A. Askar’yan, “Enhancement of transmission of laser and other radiation by soft turbid physical and biological media,” *Sov. J. Quantum Electron.* **12**(7), 877 (1982).
12. V. V. Tuchin, *Tissue Optics: Light Scattering Methods and Instruments for Medical Diagnosis*, Vol. 642, SPIE Press, Bellingham, Washington (2015).
13. T. A. Waigh, *Applied Biophysics: A Molecular Approach for Physical Scientists*, John Wiley & Sons Ltd., United Kingdom (2007).
14. V. V. Tuchin, “The optical biomedical diagnostics,” *Saratov Univ. News* **5**(1), 39–53 (2005).
15. H. Heusmann, J. Kolzer, and G. Mitic, “Characterization of female breasts in vivo by time-resolved and spectroscopic measurements in the near infrared spectroscopy,” *J. Biomed. Opt.* **1**(4), 425–434 (1996).
16. S. L. Jacques, “Optical properties of biological tissues: a review,” *Phys. Med. Biol.* **58**(11), R37 (2013).
17. W. C. Lin, M. Motamedi, and A. J. Welch, “Dynamics of tissue optics during laser heating of turbid media,” *Appl. Opt.* **35**(19), 3413–3420 (1996).
18. C. R. Simpson et al., “Near-infrared optical properties of *ex vivo* human skin and subcutaneous tissues measured using the Monte Carlo inversion technique,” *Phys. Med. Biol.* **43**(9), 2465 (1998).
19. J. J. Xia et al., “Characterizing beef muscles with optical scattering and absorption coefficients in VIS-NIR region,” *Mear. Sci.* **75**(1), 78–83 (2007).
20. A. N. Bashkatov et al., “Optical properties of the subcutaneous adipose tissue in the spectral range 400–2500 nm,” *Opt. Spectrosc.* **99**(5), 836 (2005).
21. R. Marbach and H. M. Heise, “Optical diffuse reflectance accessory for measurements of skin tissue by near-infrared spectroscopy,” *Appl. Opt.* **34**(4), 610 (1995).
22. C. P. Fleming et al., “Depth resolved detection of lipid using spectroscopic optical coherence tomography,” *Biomed. Opt. Express* **4**(8), 1269 (2013).
23. P. Wang et al., “Mapping lipid and collagen by multispectral photoacoustic imaging of chemical bond vibration,” *J. Biomed. Opt.* **17**(9), 096010 (2012).
24. V. V. Tuchin, *Lasers and Fiber Optics in Biomedical Research*, 2nd ed., Fizmatlit, Moscow (2010).
25. “Low Power CW Fiber Lasers,” IPG Group Production, <http://www.ipgphotonics.com/en/products/lasers/low-power-cw-fiber-lasers>
26. A. S. Kurkov et al., “Holmium fiber laser with record quantum efficiency,” *Quantum Electron.* **41**(6), 492 (2011).
27. S. O. Antipov et al., “Holmium fibre laser emitting at 2.21  $\mu\text{m}$ ,” *Quantum Electron.* **43**(7), 603 (2013).

**Serafima A. Filatova** has been a PhD student at the A.M. Prokhorov General Physics Institute of the Russian Academy of Sciences since 2013. Her current research interests include fiber lasers and amplifiers of 2-microns spectral range with different modes of operation, as well as laser radiation (continuous and pulsed) impact on biological tissues. She was a member of SPIE in 2013.

Biographies for the other authors are not available.